HHS Public Access

Author manuscript

J Am Chem Soc. Author manuscript; available in PMC 2017 November 23.

Published in final edited form as:

J Am Chem Soc. 2017 August 23; 139(33): 11337–11340. doi:10.1021/jacs.7b06555.

Chemically Controlled Epigenome Editing Through an Inducible dCas9 System

Tingjun Chen, **Dan Gao**, **Roushu Zhang**, **Guihua Zeng**, **Hao Yan**, **Eunju Lim**, and **Fu-Sen Liang***

Department of Chemistry and Chemical Biology, University of New Mexico, 300 Terrace Street NE, Albuquerque, New Mexico, 87131, United States

Abstract

Although histone modifications are associated with gene activities, studies of their causal relationships have been difficult. For this purpose, we developed an inducible system integrating dCas9-based targeting and chemically induced proximity technologies to allow small molecule induced recruitment of P300 acetyltransferase and the acetylation of H3K27 at precise gene loci in cells. Employing the new technique, we elucidated the temporal order of histone acetylation and gene activation, as well as the stability of the installed histone modification.

TOC image

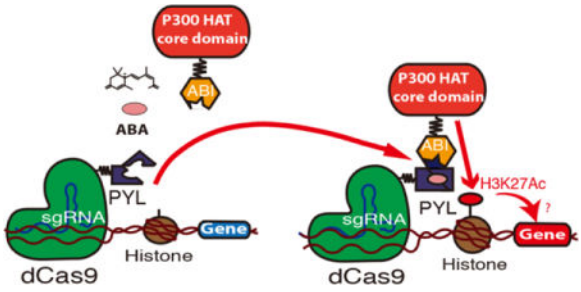

The histone tails are dynamically modified by histone modifying enzymes.[1] These epigenetic modifications alter the compactness and/or surface of chromatin to modulate interactions with transcription regulators that control gene activity.[2] It is proposed that combinations of histone posttranslational modifications (PTMs) form “histone codes” that guide gene expression.[3] Although clear correlations exist between gene activity and histone PTMs,[4] it is difficult to establish the causal relationships because tools are not available for precise temporal and gene locus specific editing of chosen histone PTMs. Because genetic or pharmacological interventions of histone modifying proteins leads to global changes in the epigenetic landscape, it is difficult to pinpoint whether a change in gene activity is a

*Corresponding Author: fsliang@unm.edu.

Tingjun Chen and Dan Gao contributed equally in this work.

Notes

The authors declare no competing financial interest.

consequence of a local epigenetic modification or secondary effects arising from changes at remote genome loci.

The CRISPR/Cas9 system has become a powerful tool for genome editing.[5] A catalytically inactive Cas9 (dCas9) enables targeting of dCas9-fused transcriptional regulators to defined genome loci by customized single guide RNAs (sgRNAs).[6] Inducible Cas9/dCas9 systems have been developed to achieve temporal control of genome editing and gene activity.[7] Although histone modifying proteins have also been fused to dCas9 to edit specific histone PTMs at chosen loci,[8] these methods lack temporal control needed to investigate the dynamics of epigenetic regulation. Herein, we describe a new small molecule inducible system that integrates chemically induced proximity (CIP)[9] and dCas9 methods to achieve temporally specific acetylation of lysine 27 on histone H3 (H3K27Ac) through gene locus specific recruitment of the catalytic acetyltransferase (HAT) domain of P300,[10] which acetylates H3K27.[11]

To develop a new technique that temporally recruits P300 HAT to a chosen gene locus, we employed the abscisic acid (ABA)-based CIP system in which ABA induces rapid binding between PYL and ABI proteins.[12] By linking PYL and ABI individually to dCas9 and the P300 HAT domain, P300 HAT can be recruited by ABA to specific genome loci targeted by customized sgRNAs (Fig. 1). Although chemical inducible systems for similar purposes have been reported,[13] they rely on genome-targeting methods that are less easily customized. Consequently, this new system employing a readily customizable dCas9-based platform should facilitate epigenome editing. The reversible nature of the ABA system[12] allows the rapid release of the recruited P300 HAT, which enables the studies on the stability and memory of the artificially established epigenetic environment.

To achieve inducible epigenome editing, we fused PYL to dCas9, tagged with a nuclear localization sequence (NLS), and a HA tag to enable chromatin immunoprecipitation (ChIP) and western blotting analysis. ABI was linked to the P300 HAT domain with a FLAG tag and NLS (Fig 2a). Both dCas9-PYL-HA and FLAG-ABI-P300 fusion proteins were expressed robustly in human HEK293T cells (Fig. S1). Four sgRNAs were used simultaneously to target the promoter region (within 200 bp from the transcription start site, TSS) of the *IL1RN* gene (Fig 2b and Table S1).[8b] The *IL1RN* locus was selected for testing in HEK293T cells because of its low H3K27Ac level and the low expression level of *IL1RN*.[8b] To monitor localization of dCas9-PYL-HA, FLAG-ABI-P300 and the level of H3K27Ac by using ChIP assays, 9 pairs of primers were designed to cover a 3.2 kb-region at the *IL1RN* locus (Fig 2b and Table S2).

To show that dCas9-PYL-HA is targeted to the *IL1RN* locus, HEK293T cells were transfected with plasmids encoding dCas9-PYL-HA with or without the co-transfection of *IL1RN*-specific sgRNAs and cultured for 24 h. Cells were then harvested and subjected to ChIP (using anti-HA antibody) and qPCR analysis in order to quantify the level of dCas9-PYL-HA at the *IL1RN* locus. The results show that, as expected, dCas9-PYL-HA is enriched over a narrow area that coincides with the sgRNA-binding locus (primer sets 4 to 6) (Fig. 2c).

To examine the recruitment of FLAG-ABI-P300, HEK293T cells were co-transfected with *IL1RN* sgRNAs, dCas9-PYL-HA and FLAG-ABI-P300 plasmids for 24 h. Cells were then either treated or not treated with 100 μM ABA for another 24 h before being harvested. Portions of the cell lysates were analyzed by using ChIP (with anti-FLAG antibody) and qPCR assays to quantify the level of FLAG-ABI-P300. We observed that the addition of ABA leads to an increase in FLAG-ABI-P300 level at the *IL1RN* locus (Fig. 2d). To determine if the level of H3K27Ac changes in response to the FLAG-ABI-P300 localization, portions of the cell lysates produced in the above experiment were subjected to ChIP (using anti-H3K27Ac antibody) and qPCR assays to quantify the H3K27Ac enrichment. The results show that H3K27Ac levels increase at the *IL1RN* locus 24 h after ABA addition, and that this increase is not observed in lysates of cells that were not treated with ABA (Fig. 2e).

To study how *IL1RN* expression levels change, total RNAs from the cell lysates generated in the above experiment were purified and then subjected to qPCR analysis to quantify mRNA levels. The results show the *IL1RN* mRNA level from cells transfected with both ABI-P300 and dCas9-PYL is similar to the level of the one from cells transfected with dCas9-PYL only. This finding suggests that the overexpression of the P300 HAT without localizing to the *IL1RN* locus did not lead to *IL1RN* expression (Fig. 2f). On the other hand, the *IL1RN* mRNA level increases when transfected cells were treated with ABA (Fig. 2f), indicating that the increase in H3K27Ac activates *IL1RN* expression. Furthermore, when a P300 mutant (D1399Y) lacking the acetyltransferase activity[8b] was used, the *IL1RN* mRNA level did not increase upon ABA addition (Fig. S2), indicating that *IL1RN* expression directly depends on H3K27 acetylation. The observations described above demonstrate that the ABA-inducible system enables installation of H3K27Ac at the *IL1RN* locus and that the consequent increase in acetylation leads to an increased level of *IL1RN* expression.

To determine if the new method is applicable to modifying H3K27Ac at other gene loci, we designed sgRNAs that target the promoter region of other genes with low expression levels in HEK293T cells, including *GRM2*, *HBA* and *MYOD1* (Table S1). The results of ChIP-qPCR assays employing primers designed to cover these gene loci (Fig. S3a, S4a, S5a and Table S2) show that in the presence of the corresponding sgRNAs, dCas9-PYL-HA is enrichment at each targeted gene locus (Fig. S3b, S4b and S5b) and ABA addition causes the enrichment of FLAG-ABI-P300 (Fig. S3c, S4c and S5c) and H3K27Ac (Fig. S3d, S4d and S5d). The level of mRNAs in each case also increases correspondingly (Fig. S3e, S4e and S5e). However, it is unclear at this moment the reasons that the observed H3K27Ac enrichment patterns were different at the 4 examined gene loci, which likely depend on the existing local epigenetic environments.

It is known that sgRNA/Cas9 can bind to unintended loci, which leads to off-target effects.[14] To examine if aberrant binding interferes with the interpretation of results, we checked all reported sites in the genome that could potentially be targeted by the *IL1RN* sgRNAs used in our studies.[15] We monitored changes in the mRNA levels of 6 genes having TSS close to the off-target sites (Table S3) after cells were co-transfected with *IL1RN* sgRNAs, dCas9-PYL-HA and FLAG-ABI-P300 plasmids followed by ABA treatment for 24 h. The observation that none of the 6 genes display increases in mRNA levels (Fig. S6) indicates that the off-target acetylation and gene activation are not significant in the studied cases. In addition,

when sgRNAs designed for *GRM2*, *HBA* or *MYOD1* were used in place of those for *IL1RN*, no increase in *IL1RN* mRNA was observed (Fig. S7), which demonstrates that the H3K27Ac enrichment at the *IL1RN* locus and gene expression are specific to *IL1RN* sgRNAs.

A significant advantage of this inducible system is that it possesses temporal control, which enables precise monitoring of the occurrence and progression of histone modification and gene expression events. To demonstrate this feature, we examined the relative timing of changes occurring in the levels of localized FLAG-ABI-P300, enriched H3K27Ac and expressed *IL1RN* mRNA after ABA induction. We confirmed that there is a significant level of sgRNA-dependent enrichment of dCas9-PYL-HA at the *IL1RN* locus at 24 h after transfection, which is the time point that we began adding ABA (Fig. S8). Within 1 h after ABA addition, FLAG-ABI-P300 is rapidly recruited to the *IL1RN* locus where it reaches a maximal level after 12 h (Fig. 3a). Correspondingly, the level of H3K27Ac begins to rise 1 h after ABA addition and continues to increase until 48 h (Fig. 3b). Finally, the mRNA level increases 4 h after ABA addition and reaches a maximum after 24 h (Fig. 3c).

The time-dependent increases of *IL1RN* mRNA, and enrichments of FLAG-ABI-P300 and H3K27Ac at each of the probed loci were subjected to nonlinear regression analysis in order to elucidate the order of FLAG-ABI-P300 localization, H3K27Ac enrichment and *IL1RN* expression. A comparison of the time periods required to reach 50% maximum enrichments shows that FLAG-ABI-P300 localization takes place before H3K27Ac enrichment and that these events are followed by *IL1RN* mRNA expression (Fig. 3d and Table S4). The same analysis for the enrichments of H3K27Ac at each probed locus revealed that a longer time is required for the level of H3K27Ac to increase at loci farthest from the FLAG-ABI-P300 site (primer 1 and 9) than the closer sites (primer 3 and 7) (Fig. S9 and Table S4). This finding suggests a possibly spreading mechanism for H3K27Ac installation from the nucleation site at the *IL1RN* locus. Whether the same spreading phenomenon exists at the other loci remains to be studied.

Another major advantage of the new ABA inducible epigenome editing system is that it is readily reversible,[12] which can be employed to remove an inducing factor rapidly so that the stability of artificially created histone PTMs can be monitored in a temporal specific manner. To determine the stability of H3K27Ac installed at the *IL1RN* locus after FLAG-ABI-P300 removal, HEK293T cells were co-transfected with *IL1RN* sgRNAs, dCas9-PYL-HA and FLAG-ABI-P300 plasmids for 24 h and then treated with ABA for another 12, 24 or 48 h. Cells were then washed with a non-ABA containing media (10 min for 3 times, or not washed as negative control) and then subjected to another 1 to 24 h culturing period. Cells were then harvested at different time points and assayed using ChIP and qPCR to monitor the levels of FLAG-ABI-P300, H3K27Ac and *IL1RN* mRNA. The results show that FLAG-ABI-P300 rapidly decreases to a near background level within 1 h following washing under all treatment conditions (Fig. 4a and S10). However, we observed that a longer ABA incubation time (48 h) increases the stability of H3K27Ac (Fig. 4b). A comprehensive time course analysis of H3K27Ac levels after ABA removal revealed that the longer cells were treated with ABA, the slower H3K27Ac was removed after washing (Fig. 4c and S10). The reasons why the stabilities of installed H3K27Ac are governed by ABA induction periods

are not known at this point. Finally, an additional experiment demonstrated that changes of *IL1RN* mRNA levels after washing under conditions described above are well correlated with the changes in H3K27Ac levels (Fig. 4d), which further confirms the causal relationship between H3K27Ac and *IL1RN* activation. We also checked the reversibility of H3K27Ac at the *GRM2* locus and observed that H3K27Ac enrichment was rapidly induced upon ABA addition and reversed after ABA removal (Fig. S11).

The last phase of this effort was aimed at demonstrating precise temporal control in histone PTM editing by this method. For this purpose, HEK293T cells were co-transfected with *IL1RN* sgRNAs, dCas9-PYL-HA and FLAG-ABI-P300 plasmids for 24 h before adding ABA. Cells were then incubated for 12 h with ABA, washed, and incubated for another 12 h period in the absence of ABA. A second dose of ABA was then added to cells, which were incubated for another 12 h before they were harvested and their H3K27Ac and mRNA levels analyzed. The results show that the H3K27Ac level can be tightly controlled temporally at the *IL1RN* locus and that the *IL1RN* mRNA levels change accordingly (Fig. S12).

In summary, we have demonstrated a new strategy, which combines the ABA-based CIP method with the dCas9 system, for temporally-controlled (both induction and reversion) and gene locus-specific editing of H3K27Ac. The observations made in this effort show that H3K27Ac leads to an increased activity of the *IL1RN* gene. We anticipate that the new strategy will be applicable to studies of other histone modifying or chromatin remodeling proteins at other target genes that are aimed at elucidating the functions and mechanisms of diverse epigenetic regulation events.

Supplementary Material

Refer to Web version on PubMed Central for supplementary material.

Acknowledgments

This work was supported by the National Institutes of Health R21 HG008776.

References

1. Berger SL. Nature. 2007; 447:407. [PubMed: 17522673]
2. Kouzarides T. Cell. 2007; 128:693. [PubMed: 17320507]
3. Strahl BD, Allis CD. Nature. 2000; 403:41. [PubMed: 10638745]
4. Zhou VW, Goren A, Bernstein BE. Nat Rev Genet. 2011; 12:7. [PubMed: 21116306]
5. (a) Jinek M, Chylinski K, Fonfara I, Hauer M, Doudna JA, Charpentier E. Science. 2012; 337(b) Cong L, Ran FA, Cox D, Lin S, Barretto R, Habib N, Hsu PD, Wu X, Jiang W, Marraffini LA, Zhang F. Science. 2013; 339:819. [PubMed: 23287718] (c) Mali P, Yang L, Esvelt KM, Aach J, Guell M, DiCarlo JE, Norville JE, Church GM. Science. 2013; 339:823. [PubMed: 23287722]
6. (a) Qi LS, Larson MH, Gilbert LA, Doudna JA, Weissman JS, Arkin AP, Lim WA. Cell. 2013; 152:1173. [PubMed: 23452860] (b) Sander JD, Joung JK. Nat Biotechnol. 2014; 32:347. [PubMed: 24584096]
7. (a) Zetsche B, Volz SE, Zhang F. Nat Biotechnol. 2015; 33:139. [PubMed: 25643054] (b) Davis KM, Pattanayak V, Thompson DB, Zuris JA, Liu DR. Nat Chem Biol. 2015; 11:316. [PubMed: 25848930] (c) Liu KI, Ramli MN, Woo CW, Wang Y, Zhao T, Zhang X, Yim GR, Chong BY, Gowher A, Chua MZ, Jung J, Lee JH, Tan MH. Nat Chem Biol. 2016; 12:980. [PubMed: 27618190] (d) Maji B, Moore CL, Zetsche B, Volz SE, Zhang F, Shoulders MD, Choudhary A. Nat Chem Biol.

2017; 13:9. [PubMed: 27820801] (e) Gao Y, Xiong X, Wong S, Charles EJ, Lim WA, Qi LS. Nat Methods. 2016; 13:1043. [PubMed: 27776111] (f) Hemphill J, Borchardt EK, Brown K, Asokan A, Deiters A. J Am Chem Soc. 2015; 137:5642. [PubMed: 25905628] (g) Zhou W, Deiters A. Angew Chem Int Ed Engl. 2016; 55:5394. [PubMed: 26996256]

8. (a) Kearns NA, Pham H, Tabak B, Genga RM, Silverstein NJ, Garber M, Maehr R. Nat Methods. 2015; 12:401. [PubMed: 25775043] (b) Hilton IB, D'Ippolito AM, Vockley CM, Thakore PI, Crawford GE, Reddy TE, Gersbach CA. Nat Biotechnol. 2015; 33:510. [PubMed: 25849900]
9. Fegan A, White B, Carlson JC, Wagner CR. Chem Rev. 2010; 110:3315. [PubMed: 20353181]
10. Delvecchio M, Gaucher J, Aguilar-Gurrieri C, Ortega E, Panne D. Nat Struct Mol Biol. 2013; 20:1040. [PubMed: 23934153]
11. Dancy BM, Cole PA. Chem Rev. 2015; 115:2419. [PubMed: 25594381]
12. (a) Liang FS, Ho WQ, Crabtree GR. Sci Signal. 2011; 4:rs2. [PubMed: 21406691] (b) Wright CW, Guo ZF, Liang FS. Chembiochem. 2015; 16:254. [PubMed: 25530501]
13. (a) Konermann S, Brigham MD, Trevino AE, Hsu PD, Heidenreich M, Cong L, Platt RJ, Scott DA, Church GM, Zhang F. Nature. 2013; 500:472. [PubMed: 23877069] (b) Hathaway NA, Bell O, Hodges C, Miller EL, Neel DS, Crabtree GR. Cell. 2012; 149:1447. [PubMed: 22704655] (c) Kadoch C, Williams RT, Calarco JP, Miller EL, Weber CM, Braun SM, Pulice JL, Chory EJ, Crabtree GR. Nat Genet. 2017; 49:213. [PubMed: 27941796] (d) Stanton BZ, Hodges C, Calarco JP, Braun SM, Ku WL, Kadoch C, Zhao K, Crabtree GR. Nat Genet. 2017; 49:282. [PubMed: 27941795]
14. Cradick TJ, Fine EJ, Antico CJ, Bao G. Nucleic Acids Res. 2013; 41:9584. [PubMed: 23939622]
15. Polstein LR, Perez-Pinera P, Kocak DD, Vockley CM, Bledsoe P, Song L, Safi A, Crawford GE, Reddy TE, Gersbach CA. Genome Res. 2015; 25:1158. [PubMed: 26025803]

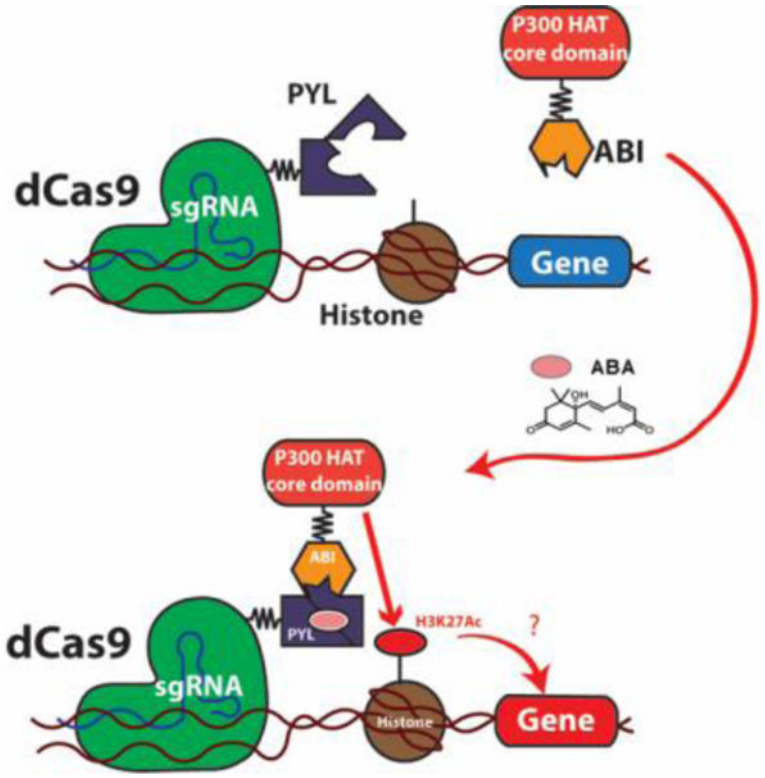

Figure 1.
Small molecule inducible acetylation of H3K27.

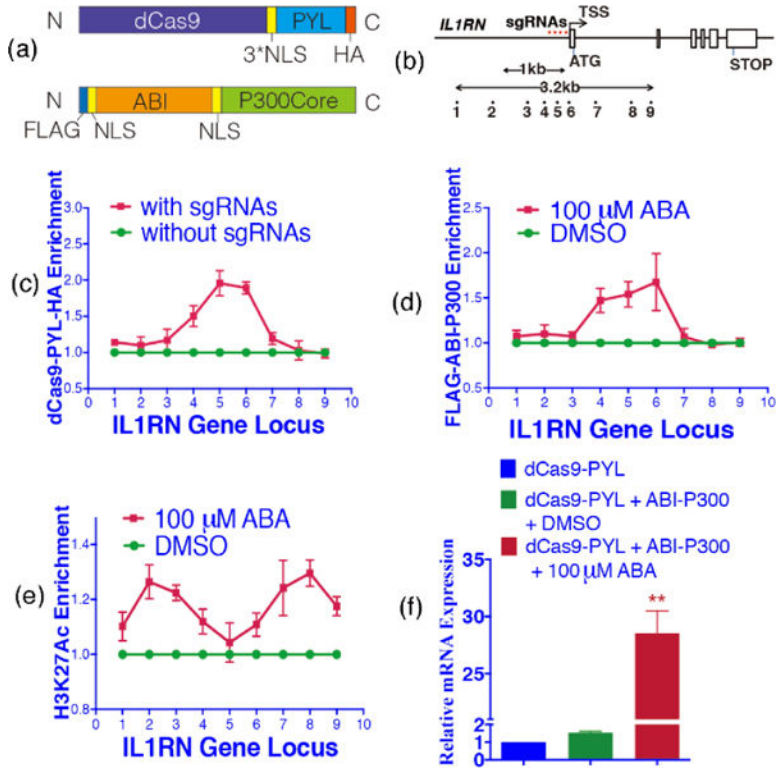

Figure 2.

Small molecule induced acetylation of H3K27 at *IL1RN* locus. (a) Constructs of dCas9-PYL-HA and FLAG-ABI-P300. (b) The sites targeted by sgRNAs (red stars) and locations probed by qPCR amplicon (black solid circles) at the *IL1RN* locus. (c) Enrichment of dCas9-PYL-HA at the *IL1RN* locus with or without sgRNAs. Enrichment of FLAG-ABI-P300 (d) and H3K27Ac (e) at the *IL1RN* locus with or without ABA treatment. (f) Levels of *IL1RN* mRNA. ** represents P<0.01 compared with control group. Fold changes were calculated by comparing to cells treated without sgRNA (c), with DMSO (d, e) or transfected with dCas9-PYL (f). Error bars represent ± s.e.m. from biological replicates (n = 5).

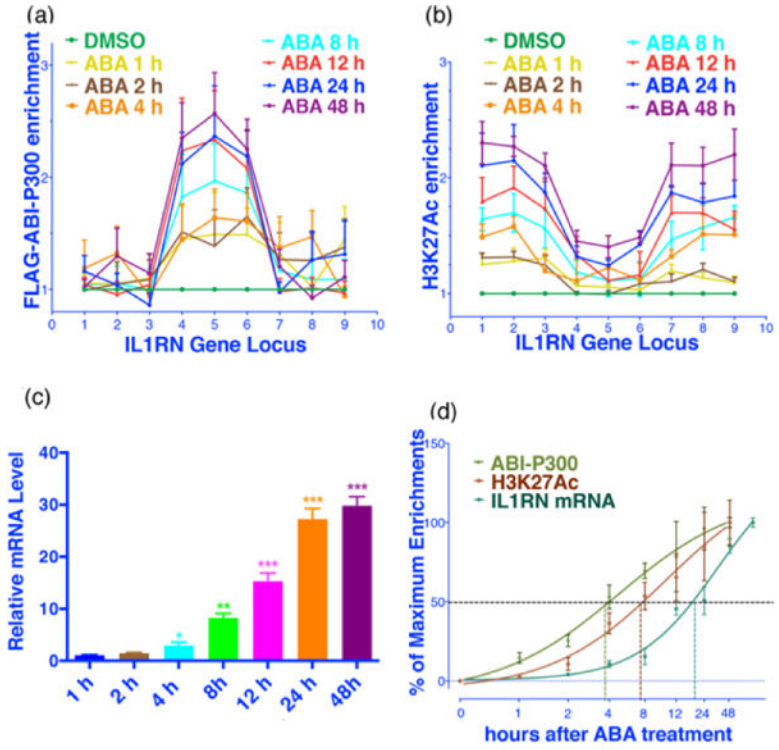

Figure 3.

The time course of H3K27 acetylation and *IL1RN* expression. Enrichment of FLAG-ABI-P300 (a) and H3K27Ac (b) at the *IL1RN* locus at indicated time points after ABA treatment. (c) Levels of *IL1RN* mRNA at indicated time points after ABA treatment. ** represents P<0.01 compared with DMSO group; *** represents P<0.001 compared with DMSO group. Fold changes were calculated by comparing to cells treated with DMSO (a, b, c). (d) The time required to reach 50% maximum enrichments of FLAG-ABI-P300 (at primer 5 locus) and H3K27Ac (at primer 1 locus) at the *IL1RN* locus, and *IL1RN* mRNA expression. Error bars represent ± s.e.m. from biological replicates (n = 6; a, b, d or 8; c).

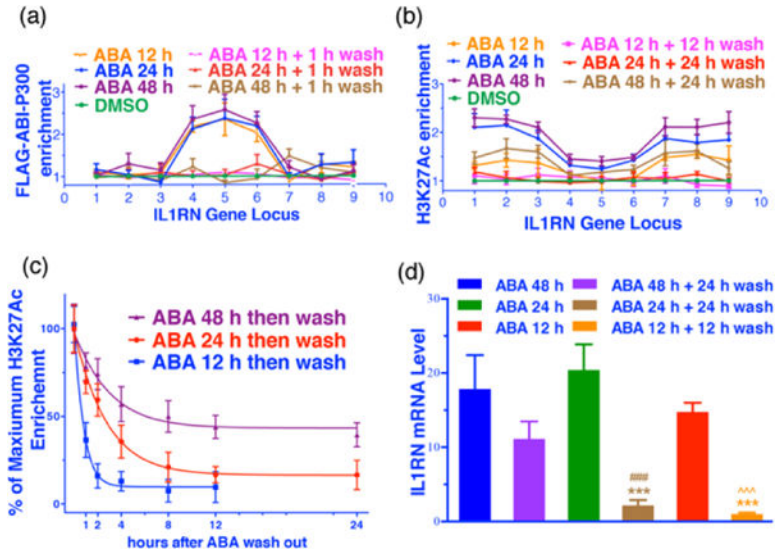

Figure 4.

The reversibility of H3K27 acetylation and IL1RN expression. Enrichments of FLAG-ABI-P300 at primer 5 locus (a) and H3K27Ac at primer 1 locus (b) at the *IL1RN* locus at indicated time points after ABA treatment with or without washing. (c) Reversing rate of H3K27Ac at the *IL1RN* locus after ABA removal. (d) Levels of IL1RN mRNA at indicated time points after ABA treatment, or after washing. ### represents P<0.001 compared with 48 h; *** represents P<0.001 compared with 24 h; ^^^ represents P<0.001 compared with 12 h. Fold enrichments were calculated by comparing to DMSO controls. Error bars represent ± s.e.m. from biological replicates (n = 6; a, b or n = 8; c).